Karthick K ✉
Magudeeeswaran G

https://doi.org/10.21278/TOF.473048822
ISSN 1333-1124
eISSN 1849-1391

EFFECTS OF GAS METAL ARC WELDING VARIANTS ON THE MECHANICAL AND MICROSTRUCTURAL CHARACTERISTICS OF AISI 304 STAINLESS STEEL

Summary

The impact of variants of gas metal arc welding on the tensile properties of AISI-304 stainless steel is presented in this article. A single V-butt joint with a groove angle of 60° and thickness of 12 mm is fabricated by four gas metal arc welding variants, such as constant current, pulsed current, double pulsed current, and cold metal transfer, under optimized conditions. The tensile properties are analysed on the cross-sectional specimen of the welded joint. The highest tensile strength of 657 MPa is recorded on the specimen welded by the cold metal transfer. The highest elongation of 19% is observed on the specimen welded by cold metal transfer, while the elongation of base metal is 45%. The results show that the joints fabricated using the cold metal transfer have superior tensile properties to those fabricated by the other three variants of the gas metal arc welding process; this is due to the electromagnetic force exerted by this welding process. The joint fabricated using the cold metal transfer process has received a low heat input, resulting in high joint efficiency and notch strength ratio.

Key words: *AISI 304 stainless steel, gas metal arc welding, cold metal transfer, pulsed current, double pulsed current.*

1. Introduction

Austenitic stainless steels (ASS) are remarkable materials for the manufacturing industries all over the world due to their adequate high-temperature mechanical properties, good weldability, high resistance to corrosion, high strength, and good ductility. Austenitic stainless steel has a primary crystalline structure and is non-magnetic with a higher density. Joining different metals or metal alloys allows you to use the properties of different materials to provide unique solutions to engineering needs [1]. The most common and well-tested structural material used for high-temperature applications in the ASS 300-series is the 304 stainless steel. The AISI 304 stainless steel is widely used in the nuclear industry, food and dairy industry [2], petrochemical industry [3], in thermal power plants [4], in the construction of shuttle tankers [5], and liquefied natural gas tankers [6].

One of the welding techniques most frequently used in the industrial sector is Gas Metal Arc Welding (GMAW), which is popular due to its inherent advantages, such as good

productivity, low cost, and simplicity in automation [7]. The GMAW process is growing in popularity in the production of stainless-steel components due to its ability to produce welds at a greater welding speed, reduced heat input, and simplicity of mechanization. In the paper [8], the authors state that GMAW is effective at increasing gap-bridging capabilities and compensating for the loss of alloy components while welding. In the GMAW process, there are typically three main, unique mechanisms of metal transfer. i.e., the short-circuiting, the globular, and the spray metal transfer. Due to recent advancements in metal transfer processes, these mechanisms are still valid, but their identities are somewhat muddled, giving rise to a number of new names for particular welding process variants [9]. The modifications have taken place in the metal transfer modes for short-circuit arc, spray arc, and pulsed arc as well. This is handled in more recent advances by including a switching frequency exceeding 100 kHz in the welding machine system, also known as the welding system frequency.

Weld quality is directly correlated with metal droplet transmission and stability during the welding process. The influence of temperature on the mechanical properties and formability behaviour of metallic materials is widely recognized. As the temperature rises, Young's modulus, yield strength, and ultimate tensile strength tend to decrease [10]. The metal transfer mode changes as the average current rises, going from the short-circuit to the globular and then the spray metal transfer mode. Spray transfer and short-circuit transfer modes are typically used for greater and lesser currents respectively; Metal Active Gas (MAG) welding is carried out at a constant current [8]. In order to solve the issue, the researchers in [11], [7], and [12] discovered that Pulsed Gas Metal Arc Welding (P-GMAW) eliminates incomplete fusion flaws and spatter while delivering a lower heat input and attaining high penetration. By keeping an eye on molten pool behaviour, it is possible to regulate welding process parameters and gather useful data that may be used to assess welding quality.

Dual pulse is also incorporated into the GMAW process to increase the efficiency of energy transmission compared to that in the pulsed and traditional GMAW processes. When compared to traditional gas metal arc welding, the dual pulsing technique reduces heat input by 67% and the amount of reverted austenite by 49% [13]. According to the paper [14], the Dual Pulse GMAW (DP-GMAW) process has a little heat input. Low frequency current pulsation is layered over high frequency pulsed current for an improved control of the arc and the metal transfer behaviour, as stated in [15]. On the other hand, using the cold metal transfer (CMT) pulse reduces the amount of ferrite as the heat input increases from 0.51 kJ/mm to 0.89 kJ/mm, resulting in a 50% reduction in the Charpy impact toughness [16]. In the study [8], the DP-GMAW technique was used to weld aluminium alloy AA5754. According to the earlier work described in [14] and [17], the DP-GMAW method is carried out with a lower heat input than those of the standard and pulsed GMAW techniques. It is widely accepted that increasing the heat input promotes chromium depletion. As a result, the welding grade AISI 310S ASS material requires extra care [18].

In 2004, "Fronius of Austria" developed CMT welding, an improved version of the traditional GMAW/MIG (Metal Inert Gas) method that is based on short-circuiting transfer and differs from other GMAW processes [11]. As the name implies, "cold" refers to the fact that this is the only method of fusion welding that uses a minimum thermal heat input, owing to a very low non-zero current [19]. The CMT welding process allows a regulated way of material deposition with minimum thermal heat input by combining an improved wire feeding mechanism with quick digital monitoring [20]. The integration of wire movement is the primary innovation of CMT. The digital process control regulates the movement of the wire retraction and forces the power supply when a short circuit develops. When a short circuit occurs, the liquid metal droplet on the wire's tip is urged to separate by the motion of the wire being retracted. In the CMT welding, one-fourth of the entire time is spent in the short-circuit phase, when the amplitude of the current is close to zero. It is an energy-efficient welding process

since it significantly lowers welding costs and energy consumption by 30% to 40%. In contrast to MIG welding, electromagnetic force has no effect on the transmission of liquid metal droplets in a short circuit, resulting in a significant decrease in the heat input and weld spatter [21]. Due to the wire retraction motion of the CMT, which is controlled by digital process control, the current waveform in the CMT is low and constant, while the voltage waveform is nearly zero and constant. This promotes heat input reduction and spatter-free welding. In the current situation, new developments in welding techniques are replacing traditional welding techniques for industrial and advanced technical applications. The use of CMT, a more advanced form of MIG welding, is now widespread due to its improved bead aesthetics, minimal spatter formation, and decreased heat input. Due to these qualities, CMT is unique in its applications. Today, CMT is used in additive manufacturing via Wire-Arc Additive Manufacturing (WAAM). The application of nickel titanium (NiTi) alloys will be substantially aided by the good heat management of the CMT process and the optimization of depositing speed [22]. Due to the minimal dilution, using the cold metal transfer method is a great solution for nickel-based alloys on oil and gas pipelines [23].

The study [24] presents the "mechanically-aided droplet deposition", a short-circuit control technique; the technique involves withdrawing the wire from the short-circuiting area. In contrast to the traditional MIG process, the droplet detachment mode in the CMT process does not rely on electromagnetic force, which lowers spatter [21]. According to [25], due to a low heat input and little distortion, the CMT process is particularly well suited for welding thin aluminium alloy sheets. The low heat input prevents the development of brittle intermetallic compounds [25], [26]. Some of the latest non-destructive methods carried out on CMT weld samples include quantitative infrared analysis. The studies[20], [27], and [24], present a model that is important for modelling the specific interactions between the wire feeding and heat input. Digital process control in the CMT process reverses the servomotor of the "robacter drive" welding torch when the electrode wire tip touches the molten pool. As a result, the wire retracts, encouraging the droplet transfer. The current decreases almost to zero during the metal transfer, preventing the creation of any splatter. The arc will be restarted, and the wire will be fed forward again with a pre-set welding current reflowing once the metal transfer is finished [28]. The amount of time needed for a droplet of molten electrode to deposit into the weld pool can be referred to as a standard CMT welding electrical signal cycle. An analysis of voltage and current waveforms is necessary to comprehend how much energy is distributed throughout each phase of the droplet transfer process [29].

According to experiments done and presented in [30], the CMT process has various advantages over typical MIG welding, including low energy consumption, spatter-free operation, and rapid welding. With lap joints in particular, there is a significant risk of partial fusion, which could be reduced by lengthening the arc. Compared to traditional MIG welding, CMT welding demonstrated greater stability and a better finish on the surface and under the joints [31]. Weld bead porosity production was less likely to occur under low and high heat input conditions, while it was more likely to occur under medium heat input levels. Small porosities at the weld root were caused by early solidification under low heat input conditions, which are prevented under high heat input conditions in CMT [32]. According to [25], the CMT increased the strength of the dissimilar metal lap connection by lowering the thickness of the brittle intermetallic compound at the interface between steel and aluminium. In the CMT method, the length of the arc may be easily checked and controlled mechanically. As a result, the arc has perfect stability, regardless of the surface being joined or the joining speed, making it possible to use the CMT welding technique in any position and for every purpose [33].

The joints thus created exhibits relatively low porosity, no splatter, and no cracks. When compared with the base metal, the joints showed a minimal micro-hardness in the weld zone and a small hardness reduction in the heat affected zone. The joints fabricated by the CMT

welding process had superior mechanical strength compared to those produced by traditional MIG and TIG (Tungsten Inert Gas) techniques and were on a par with those created by the friction stir welding and laser beam welding methods. When compared to the joints produced by traditional MIG welding, the CMT joints have smaller HAZ and the residual stresses are shown to be minimal. The crystallites in the weld zone are identical in size and geometry to those produced by the traditional MIG technique. The homogeneity of the weld bead has not shown any appreciable variation during the energy dispersive spectroscopy chemical analysis. According to [32], the CMT welding is the best type of welding.

It is generally known that the microstructure of 304 stainless steel is mainly composed of austenite (γ-Fe) under the condition of equilibrium solidification. However, the high cooling rate under the non-equilibrium fast solidification condition will lead to an incomplete δ-γ transition, and some metastable δ-Fe must be kept indefinitely [15], [17]. The ferrite-to-austenite ratio in the 304 stainless steel welding process is widely known to be heat-dependent. It has been found that the microstructure of a joint has a significant impact on the mechanical characteristics of stainless steel.

However, only few reports are available on the mechanical characteristics of austenitic stainless steel (AISI 304) joints fabricated using the DPC-GMAW and CMT-GMAW processes. The austenitic stainless steel AISI 304 has been traditionally welded by constant current GMAW and pulsed current GMAW in industrial applications. The double pulsed GMAW and the cold metal transfer mode of GMAW have not been investigated and used for joining AISI 304 so far. From the literature, it is understood that researchers have not explored the variants of GMAW with high thickness materials. Although some of the authors have considered some variants, such as constant current and pulsed current, but have not considered all the variants dealt with in this study, i.e., double pulse current and cold metal transfer. This research gives an insight into and a good understanding of the mechanical properties which may provide ease and confidence in the wide use of the DP-GMAW and CMT processes to produce welds of desired quality. The CMT method used for joining AISI 304 stainless steel plates imparted lower heat input when compared with other modes of metal transfer considered in this study. The application of the CMT method resulted in superior mechanical properties and metallurgical characteristics of the welded joints.

2. Experimental Work

AISI 304 plates of 12 mm thickness are used as the base metal. The plates have a 60° single V-groove angle; their dimensions are 300 x 75 mm. The AISI 304 plates are wire-brushed to remove the oxide layer and then wiped using acetone. The filler wire used is the ER308 L wire with a diameter of 1.2 mm. A gap of 0.8 mm is maintained between the plates.

Table 1 Chemical components (wt %) of the base metal and filler wire

Material	C	Mn	P	S	Si	Cr	Ni	Mo
AISI 304	0.08	2	0.045	0.03	1	19	10	-
ER308L	0.03 max	1.0-2.5	0.03 max	0.03 max	0.30-0.65	19.5-22.0	9.0-11.0	0.75 max

Table 2 Mechanical properties of the base metal

Grade	Tensile strength (MPa)	Compression strength (MPa)	0.2% proof stress (MPa)	Elongation A5 (%)	Charpy impact energy (J)
AISI 304	520	210	210	45	248

The chemical components of the filler wire and base metal are given in Table 1 and the mechanical properties of the base metal are given in Table 2. The shielding gas used for this experimental study is Argon (99.99 wt%), which is maintained at a flow rate of 15l/min.

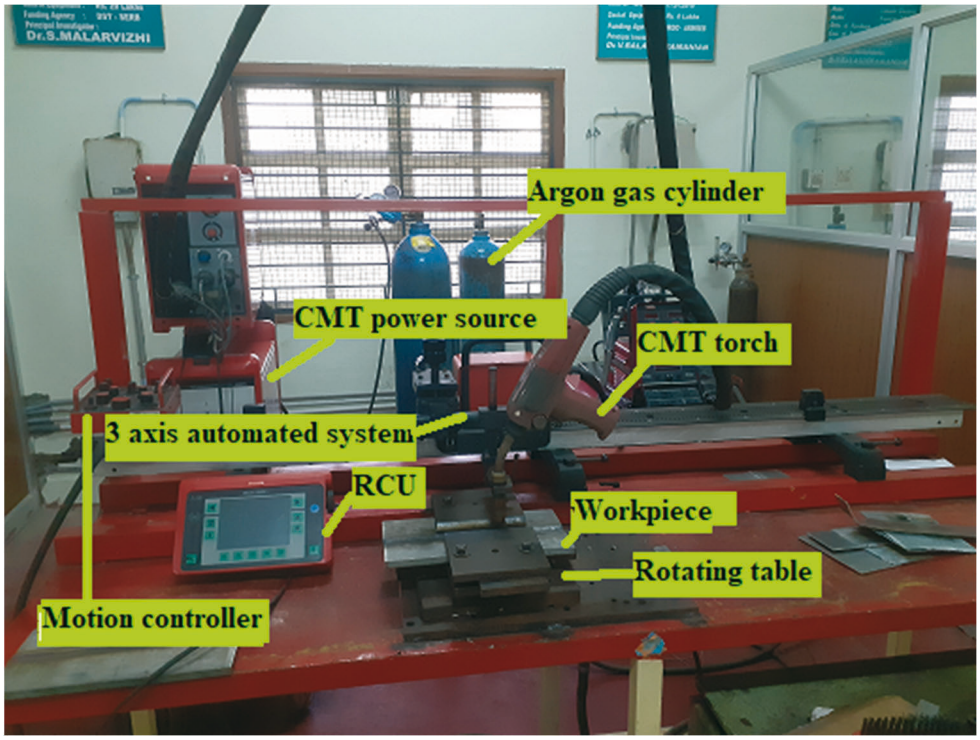

Fig. 1 A Photograph of a cold metal transfer (CMT) welding machine

Figure 1 shows the CMT machine used to fabricate joints. The experiment has been carried out using different variants of GMAW. The variants used here are Constant Current-GMAW (CC-GMAW), Pulsed Current-GMAW (PC-GMAW), Double Pulsed Current-GMAW (DPC-GMAW), and Cold Metal Transfer-GMAW (CMT-GMAW). For each GMAW variant, three joints were produced and nine samples of tensile, notch tensile, and impact specimens were made from each variant and tested according to the standards; the standard deviations are given in Table 4.

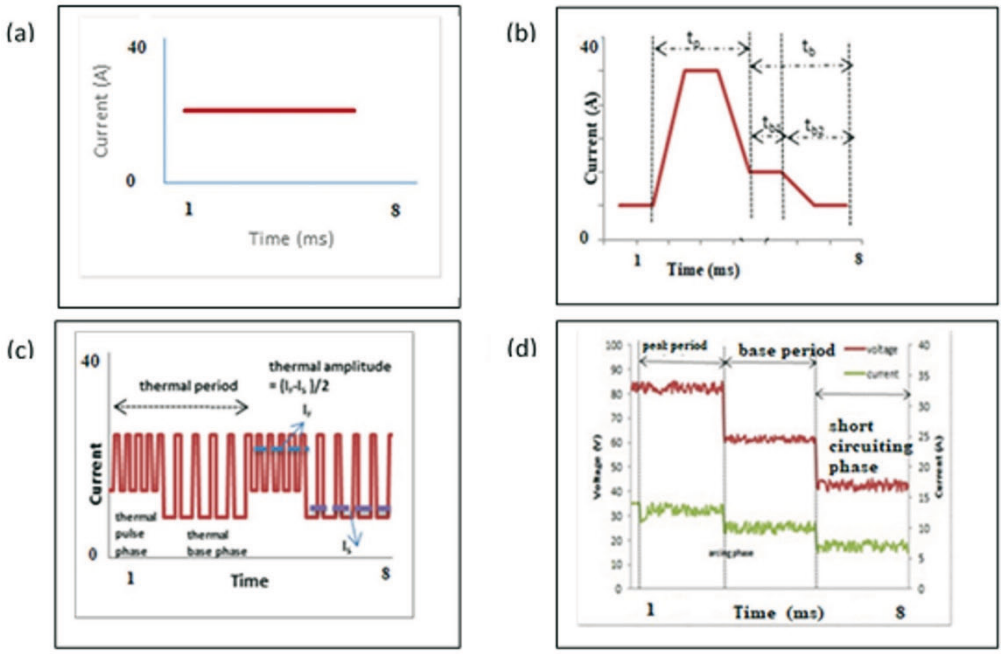

Fig. 2 Wave patterns of the GMAW variants (a) CC-GMAW (c) DPC-GMAW (b) PC-GMAW (d) CMT-GMAW

Table 3 Welding parameters used for joint fabrication

Variant	Welding current (A)	Arc voltage (v)	Arc length correction (%)	Wire feed speed (mm/min)	Pulse frequency (Hz)	Welding speed (mm/min)	Heat input (kJ/mm)
CC-GMAW	135	24.5	0	4800	-	116.3	1.71
PC-GMAW	87	23.5	0	3700	350	120	1.02
DPC-GMAW	82	19.5	0	3200	410	128.57	0.75
CMT-GMAW	108	16.1	0	6400	-	151.26	0.69

Note: PC-GMAW: I_b=65 A, t_b=2.035 ms, I_p=205 A, t_p=0.814 ms; DPC-GMAW: I_b=61.3 A, t_b=1.735 ms, I_p=193, t_p=0.694 ms. Stick-out length = 0.75 inches, torch angle = 30°, preheat temperature = 100°, interpass temperature = 150°.

The wave patterns of the GMAW variants are shown in Fig.2. Table 3 shows a list of welding specifications used to create the joints. Additional parameters, such as base current *(I_b)*, base time *(t_b)*, peak current *(I_p)*, and peak time *(t_p)*, are considered for the pulsing and double pulsing modes. Some other parameters, such as stick-out length, torch angle, preheat temperature, and interpass temperature, are also considered for all four variants of GMAW. The stick-out length is the distance between the end of the electrode and the tip of the welding gun. A proper stick-out length ensures good electrical conductivity and stable arc formation. We used a stick-out length of 0.75 inches. If the stick-out length is too short, the arc may become unstable and cause excessive spatter; and if it is too long, it can result in poor arc stability, wire burnback, and incomplete fusion. Thus, the stick-out length is an important parameter that can affect the quality and stability of the welding process. The torch angle refers to the angle of the welding gun with respect to the workpiece. A proper torch angle ensures good penetration, proper fusion, and reduced spatter. A torch angle of 30 degrees is used here. If the angle is too low, it can result in poor penetration and incomplete fusion, while a too wide torch angle can cause excessive heat input and distortion. The interpass temperature is the temperature of the workpiece between each pass of welding. It is important for the control of excessive heat input, distortion, and cracking. A proper interpass temperature helps to ensure good fusion, reduce the risk of solidification cracking, and maintain the desired mechanical properties of the welded joint. The interpass temperature of 150°C is maintained here. If the interpass temperature is too low, it can cause the formation of cold cracks, while a temperature that is too high can lead to distortion. Consequently, the interpass temperature is an important parameter that can affect the mechanical properties of a welded joint. Preheat temperature is the temperature of the base material before welding. It is used to reduce the temperature gradient and thermal stresses in the weld zone and adjacent material, improve the weldability of the base material, and reduce the risk of cracking. Here, a preheat temperature of 100°C is used, which helps to reduce the risk of thermal cracking and improve the weldability of the base metal.

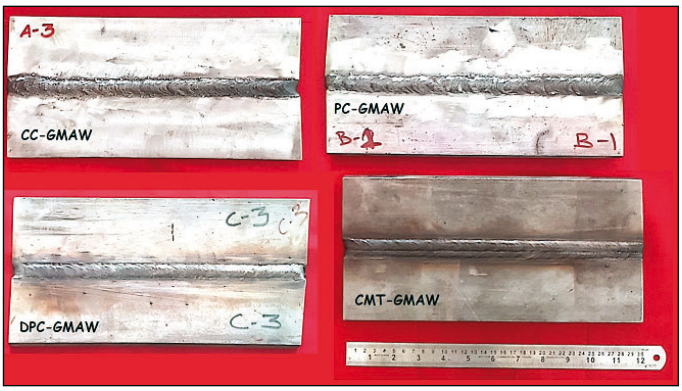

Fig. 3 Images of the welded joints

Figure 3 shows the images of the welded joints. The heat input (HI) is given by,

$$\text{HI} = \frac{\eta * V * I * 60}{S * 1000} \text{ kJ/mm} \quad (1)$$

where V, I, S, and $\eta = 0.8$ represent the arc voltage, arc current, welding speed, and thermal efficiency constant, respectively.

$$\text{Arc current} = \frac{I_b t_b + I_p t_b}{t_b + t_p} \quad (2)$$

$$\text{Pulse Frequency} = \frac{I}{t_b + t_p} \text{ Hz} \quad (3)$$

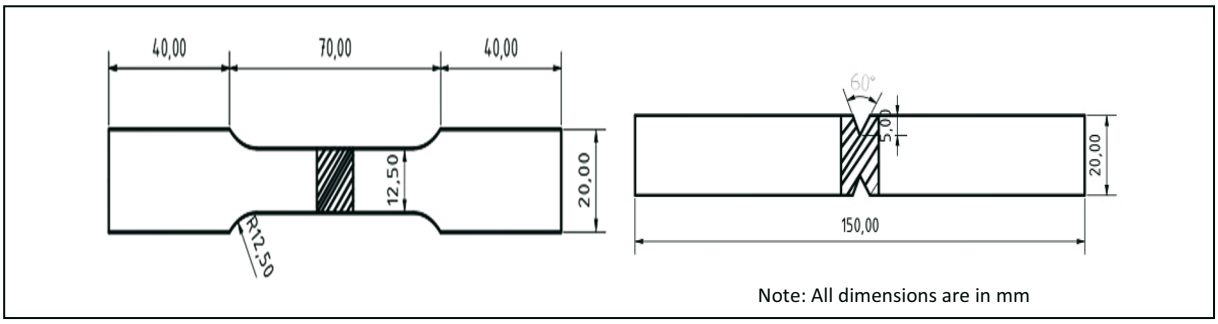

Fig. 4 Dimensions of the smooth and notch tensile specimens

Before specimen testing, the joints welded by using all the variants are inspected by a liquid penetrant test; it is confirmed that the welded joints have no visible flaws. Figure 4 shows a schematic representation of a smooth and a notch tensile specimen. An electrolytic etch test is carried out according to the ASTM E262 practice A, using the etchant acidic solution comprising 100 g of reagent-grade oxalic acid ($H_2C_2O_4.2H_2O$) and 900 ml of distilled water. Scanning Electron Microscopy (SEM) is used to characterize the microstructure of different zones. In order to prove that the mechanical properties of specimens welded by the CMT are superior, the specimens welded by other variants of GMAW must undergo tensile and impact tests.

3. Results

3.1 Tensile properties

In all of the variants, fractures are seen in the welded region. The lowest tensile strength of 620 MPa is noted in the CC-GMAW joint. The base metal exhibits a 45% elongation. Among the four types of specimens, the lowest elongation of 10.6% is noted in the CC-GMAW joint, whereas the maximum elongation of 19% is noted in the CMT-GMAW joint. The tensile strength of 624 MPa is observed in the PC-GMAW joint, which exhibits a 16.2% elongation. The results of CMT-GMAW clearly show that the elongation is reduced 42.22% in comparison with the base metal.

Table 4 Tensile properties of the welded joints

Joint Type		0.2 % yield strength (MPa)	Ultimate tensile strength (MPa)	Elongation in 50 mm gauge length (%)	Notch tensile strength (MPa)	Notch strength ratio	Joint efficiency (%)	Fracture location
CC-GMAW	Mean	452	620	10.6	634	1.022	77.9	Weld
	SD	3.33	5.69	0.32	4.59			

Joint Type		0.2 % yield strength (MPa)	Ultimate tensile strength (MPa)	Elongation in 50 mm gauge length (%)	Notch tensile strength (MPa)	Notch strength ratio	Joint efficiency (%)	Fracture location
PC-GMAW	Mean	460	624	12.8	641	1.027	78.4	Weld
	SD	4.4	4.94	0.58	5.37			
DPC-GMAW	Mean	467	638	16.2	655	1.026	80.2	Weld
	SD	5.26	5.83	0.39	4.66			
CMT-GMAW	Mean	485	657	19	678	1.03	82.6	Weld
	SD	5.45	5.31	0.8	5.19			

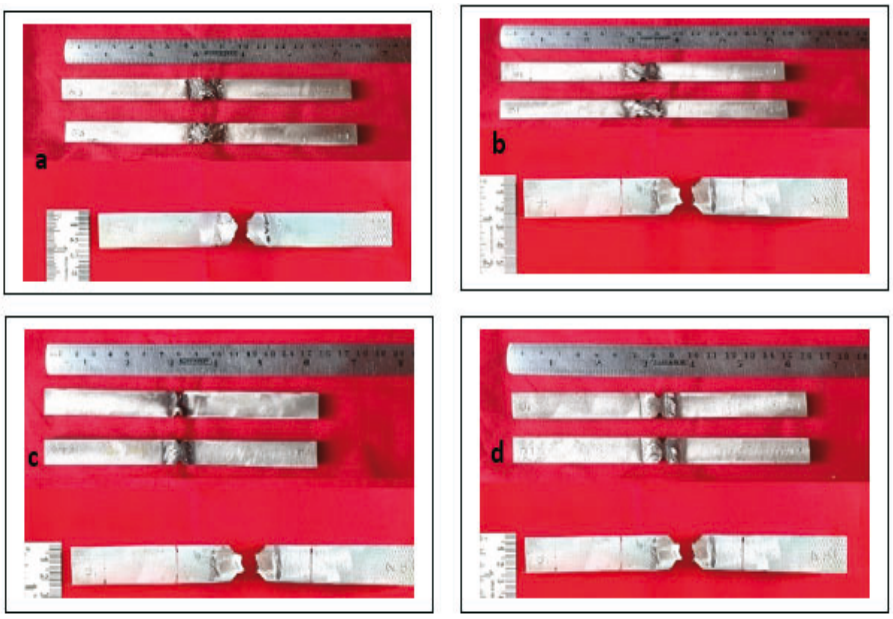

Fig. 5 Locations of the notch tensile fracture in specimens before and after the test: (a) CC-GMAW; (c) DPC-GMAW; (b) PC-GMAW; and (d) CMT-GMAW

Fig. 6 Locations of tensile fracture in specimens before and after the test (a) CC-GMAW; (b) PC-GMAW; (c) DPC-GMAW; and (d) CMT-GMAW

Table 4 shows the tensile properties of the average of three welded specimens. The Notch Tensile Strength (NTS) and the Notch Strength Ratio (NSR) of a notched specimen are obtained by performing a standard tensile strength test. The NSR is defined as the ratio of tensile strength of the notched specimen to the tensile strength of the unnotched specimen. It has been noted that the CMT-GMAW specimen is marked with the highest NTS value of 678 MPa and the CC-GMAW specimen with the lowest NTS value of 634 MPa. All the variants are observed to have the NSR value greater than 1; however, the NSR value of the CMT-GMAW specimen is higher than those of other variants. From this it follows that the joints become less sensitive to notches and fall into the category of joints characterized by notch ductility. Joint efficiency, which is defined as the ratio of the tensile strength of the joint to the tensile strength of the base metal, is another important factor that determines the good quality of the joint. The locations of notch tensile fractures and tensile fractures in specimens are shown in Fig. 5 and Fig. 6, respectively.

3.2 Macrostructure and microstructure

The four GMAW variants, CC-GMAW, PC-GMAW, DPC-GMAW, and CMT-GMAW, produced full-penetration welds. The width and the fusion area of the four joints differ from one another. Different welding speeds and heat inputs used in the four welding processes are responsible for the differing widths and fusion areas.

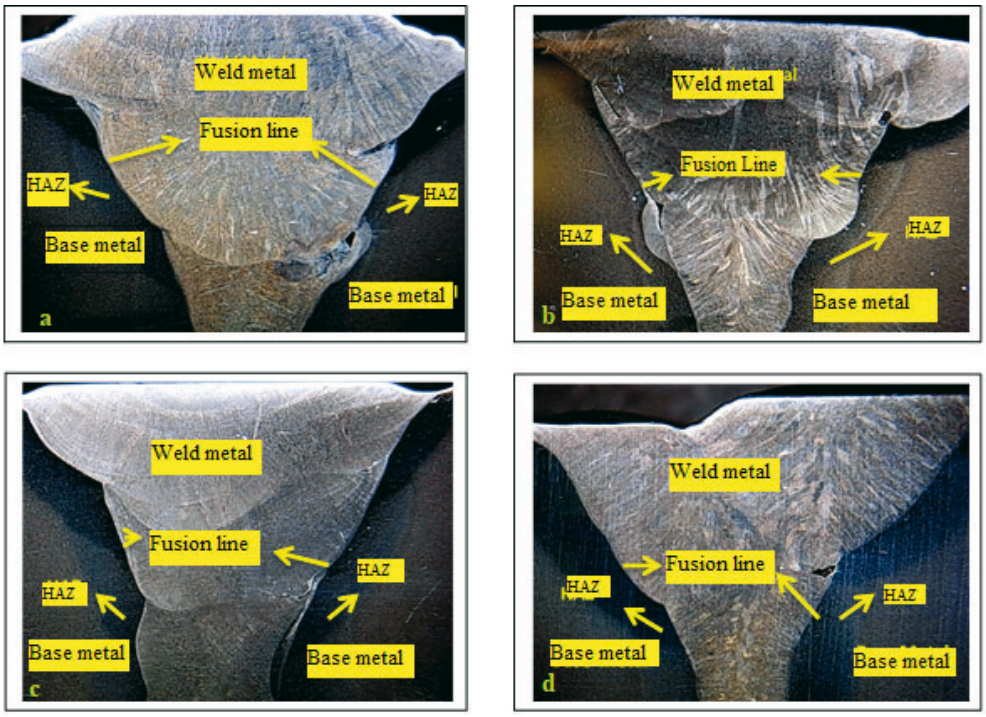

Fig. 7 Macrograph (10 mm) of the heat affected zone (HAZ) (a) CC-GMAW, (b) PC-GMAW, (c) DPC-GMAW, (d) CMT-GMAW

Weld pads were used to create a specimen, as shown in Fig 7, in order to detect the microstructural changes related to various welding processes that take place during welding. To make it easier to measure the details, such as the cross-sectional areas of the heat-affected and fusion zones, the cross-sections of the weld joints were taken after polishing and macro-etching with the aid of a microscope at a magnification of 10. General microstructural observations were made using conventional polishing techniques. With the aid of an optical microscope and image analysis software, the microstructures of various zones of interest, including the weld metal, heat-affected zone, and interface region, were observed and photographed.

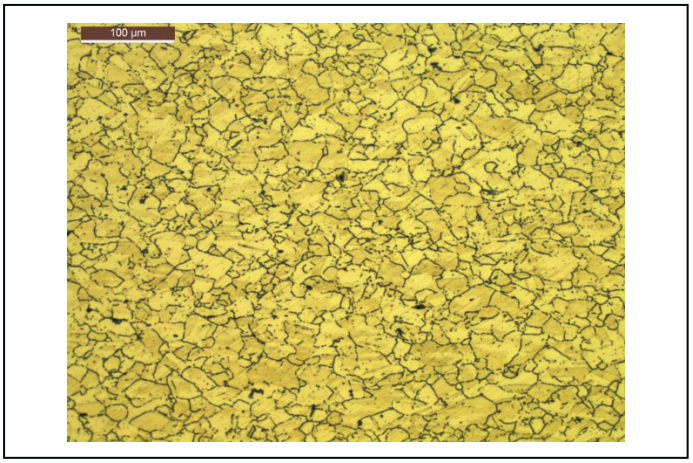

Fig. 8 Micrograph of the base material, AISI 304 stainless steel

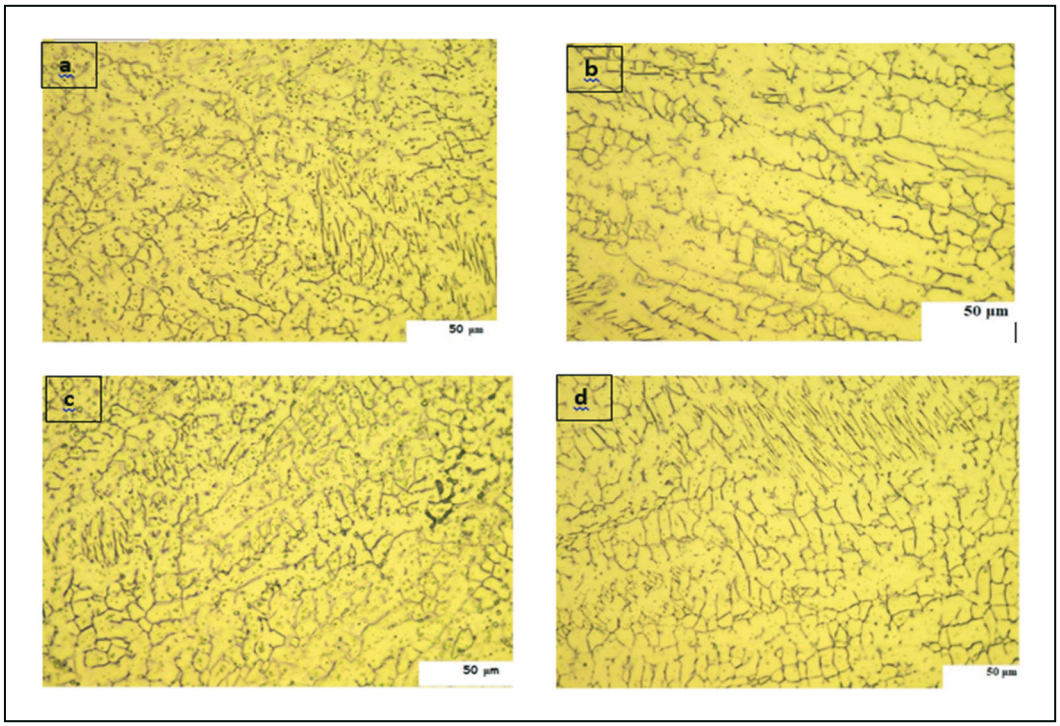

Fig. 9 Optical micrographs of the weld joint region: (a) CC-GMAW (b) PC-GMAW (c) DPC-GMAW (d) CMT-GMAW

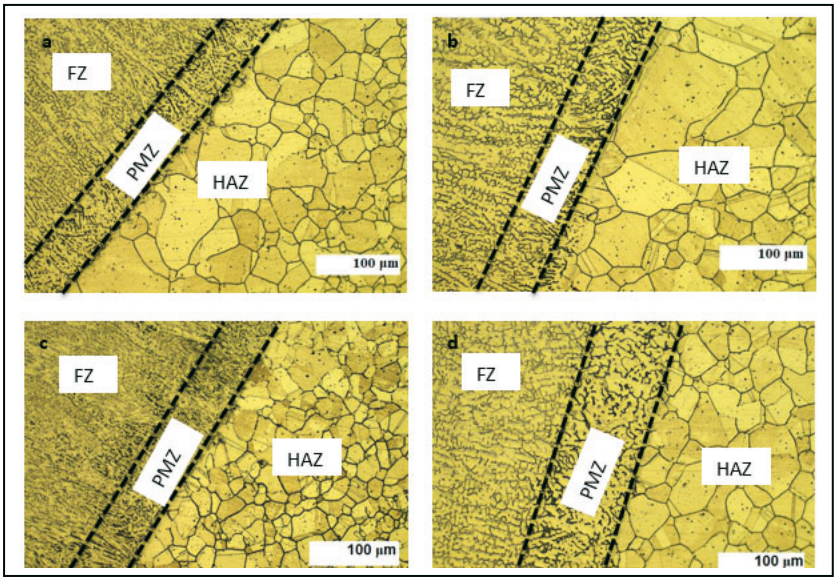

Fig. 10 Optical micrographs of the interface region (a) CC-GMAW (b) PC-GMAW (c) DPC-GMAW (d) CMT-GMAW. Note: FZ-fusion zone; PMZ-partially melted zone; HAZ-heat-affected zone

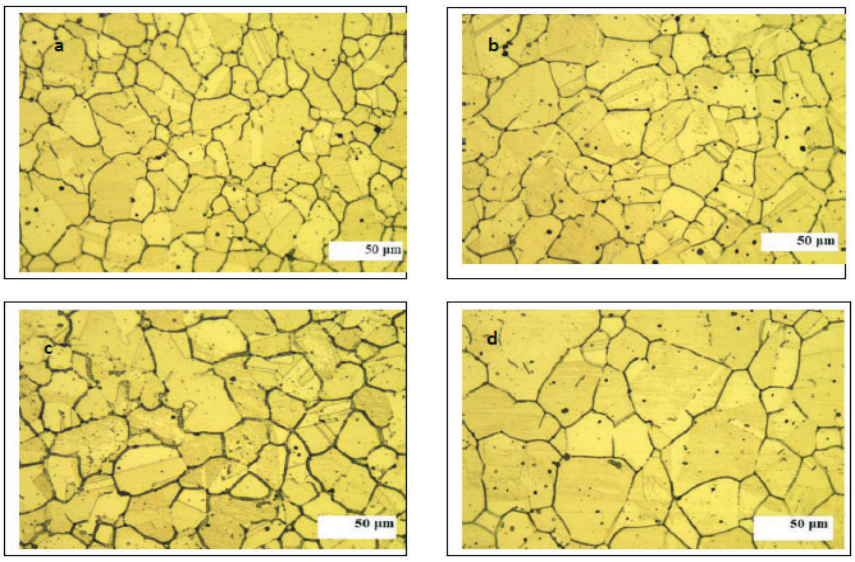

Fig. 11 Optical micrographs of Heat Affected Zone (a) CC-GMAW, (b) PC-GMAW, (c) DPC-GMAW, (d) CMT-GMAW

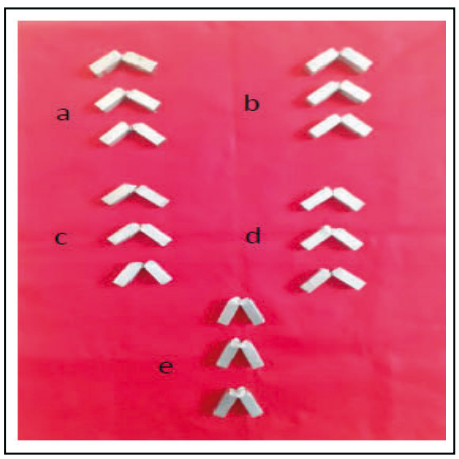

Fig. 12 Impact strength (a) CC-GMAW, (b) PC-GMAW, (c) DPC-GMAW, (d) CMT-GMAW, (e) Base metal

An IT-30 (*ASTM*) 300 Joule impact tester was used to conduct Charpy V-Notch (CVN) tests, which are used to analyse the material toughness and ductility. According to the ASTM E23 standard specification, welded joints were used to create test specimens for the Charpy impact. The specimens for this investigation were wire-cut transversely to the weld. Impact test specimens were made by etching them with 2 percent nital to reveal the contour of weld metal, heat-affected zone, and base metal in order to confirm the location of the Charpy V-notch. The location of the impact test specimen V-notch was identified at the weld metal, HAZ, and base metal to assess the toughness at a particular point.

A micrograph of AISI 304 stainless steel is shown in Fig. 8. Optical micrographs of welded joint region, interface region, and HAZ of four GMAW variants, i.e., CC-GMAW, PC-GMAW, DPC-GMAW, and CMT-GMAW, are shown in Fig. 9, 10, and 11, respectively. Figure 12 shows the impact strength of the four GMAW variants and the base metal.

4. Discussion

Without any splatter, the pulsed current welding process lowers the overall heat input. This particular form of constant current welding involves pulsing the welding current from high to low at a set frequency. The joint made with the CMT-GMAW process had a maximum tensile strength of 657 MPa. It is due to a short circuit, which reduces the welding current and retracts the weld wire, resulting in a drop-by-drop deposit of weld material. In contrast, the weld made with the CC-GMAW process had the lowest tensile strength of 620 MPa. Heat treatment is critical in improving the mechanical properties of welded joints. The transverse tensile test results indicate that all specimens failed at the weld metal, regardless of the modes of metal transfer used to fabricate the joints. The presence of lightened precipitates is the cause of the failure in the weld metal region. When compared with the CC-GMAW and PC-GMAW joints, the CMT-GMAW joint has faster cooling rates, which affects several aspects of weld metal solidification.

The optical micrographs show that the dendrite size and the interdendritic spacing in the weld metal increase as the heat input decreases. When the heat input is low and the cooling rate is relatively high, dendrites have less time to develop because of the steep thermal gradients that are created in the weld metal. This accounts for the difference in the dendrite size. When the heat input is high, the cooling rate is slow; this gives the dendrites more time to grow into the HAZ.

As shown in Fig. 10, the weld zone primarily consists of columnar dendrites. In GMAW, the super-cooling taking place at the solid-liquid interface in GMAW expands in a perpendicular direction to the edge of the fusion line; this causes the material to solidify quickly. The image shows variations in grain development in the melt puddle as a result of cooling time. The improvement in the overall fusion structure is brought about by different cooling times, which also improve mechanical properties, such as tensile strength, fracture resistance, and stress. The microstructure changes as a result of the fluctuation in time, which is dependent on the cooling speed. The grain structure is anisotropic, as shown in [10]; it assumes a columnar shape towards the heat flux that is roughly normal to the direction of welding.

Due to the decreased heat input required for this process, the microstructure clearly shows that the width of the HAZ and that of the partially melted zone (PMZ) are smaller in the CMT-GMAW joints and are roughly equal to that in the DP-GMAW ones. Weld metal has a slightly greater hardness than the metal in the HAZ, even if precipitation is fully dispersed in the weld metal zone. This implies that fracture may occur in the HAZ, where the softened zone occurs, regardless of the GMAW type. The softened zone in the HAZ frequently occurs because of the coarsening of harder precipitate when an alloy is subjected to higher peak temperatures. The hardened and unstable harder precipitate may have partially dissolved or coarsened, causing the

lowest hardness of the softened zone. Regardless of the variant employed, the weld metal zone had the greatest hardness recorded. Depending on the variant used, the width of the softened zone varies. It is obvious that the width will change according to the amount of heat generated by each of welding processes. The CMT-GMAW joint exhibited a rigid hardness of 79 HV in the weld metal zone. This is because this process has a low heat input (0.69 kJ/mm) with recrystallization and rapid cooling rate when compared with the other three variants.

Typical micrographs of the welded area of the four joints are shown in Figure 9. A dark δ-Fe dendritic structure in an austenite matrix can be noted in all joints; however, dendritic sizes vary. The PC-GMAW joints have obviously greater δ-Fe dendritic sizes than the other three joints. The smallest dendritic size of all four joints is exhibited in the CC-GMAW joint. Additionally, the δ-Fe in the PC-GMAW joint has a columnar structure, but in the CMT joint, it appears as a network morphology in the fusion zone. The solidification proceeds in a specific direction during the CC-GMAW process. In comparison to other joints, the CC-GMAW joints contain more phases in the weld metal area. In addition, the fractured area of the CC-GMAW joints has a lower area allocation of dimples with huge diameters. This is because of the extremely high heat input (1.71 kJ/mm) of the CC-GMAW. This results in lesser mechanical properties of the CC-GMAW joints. The arc pressure and stiffness in the PC-GMAW process are primarily determined by the pulse frequency and peak current. As a result, when compared to the CC-GMAW process, PC-GMAW is distinguished primarily by pulse frequency and peak current, which aid in refining the columnar grain structure. The transmission of phases in the PC-GMAW joints is reduced in comparison to that in the CC-GMAW joints due to the low heat input (1.02 kJ/mm).

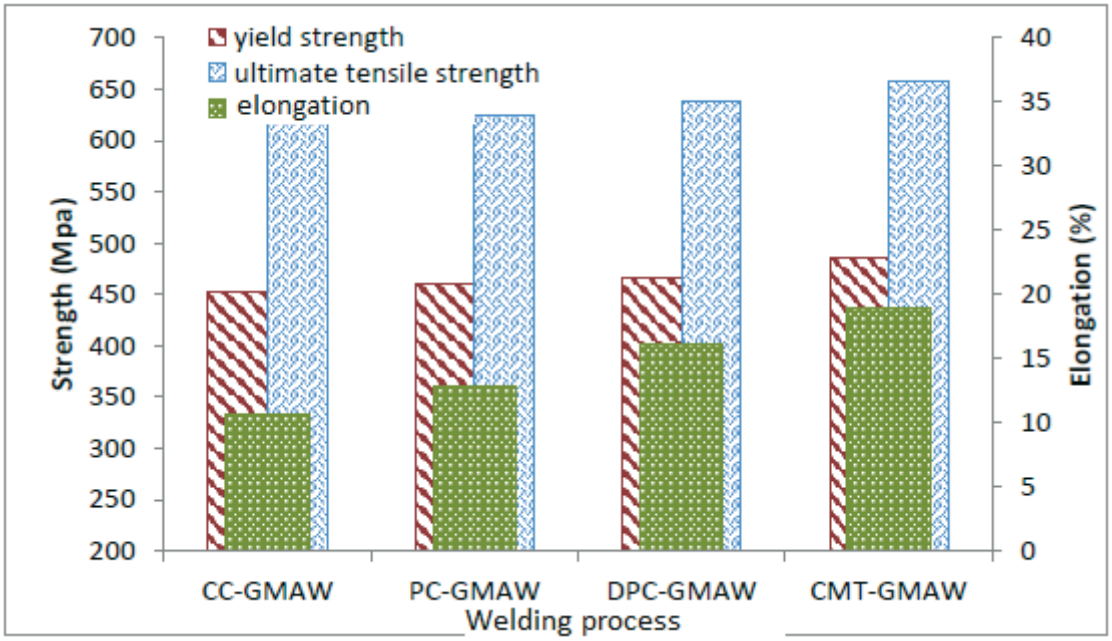

Fig. 13 Tensile properties of weld metal for four variants of GMAW

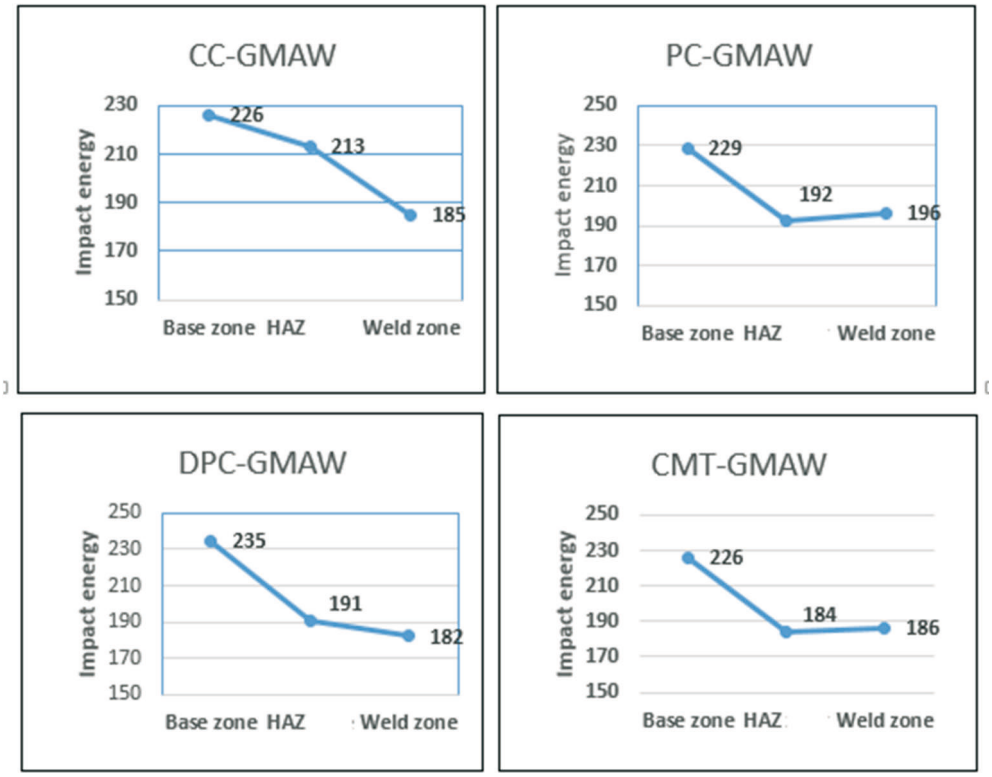

Fig. 14 Impact energy (Joules) for variants of GMAW process in various locations (Base zone, HAZ, and Weld zone)

From Fig. 13, it is evident that the tensile properties of CMT-GMAW are comparatively better than those of the other three variants. Although the improvisations in yield strength and ultimate tensile strength are minimal, the elongation of the CMT-GMAW shows a maximal difference compared to other variants. Figure 14 shows the impact energy of all four variants.

5. Conclusions

Following are the important conclusions made through this investigation:

1. Constant current (CC-GMAW), pulsed current (PC-GMAW), double pulsed current (DPC-GMAW), and cold metal transfer (CMT-GMAW) processes all achieved full-penetration joints free of flaws. All joints have the δ-Fe phase and γ-Fe phase microstructures.
2. Due to a lower heat input of the CMT-GMAW process than those of other three processes, the CMT joints showed less softening in the HAZ than other variants.
3. From the investigations conducted on four variants of GMAW, one can note that the CMT-GMAW joint exhibits high tensile strength and notch tensile strength due to its faster cooling rate.
4. Due to a low heat input, the CMT-GMAW process has a smaller HAZ and a smaller partially melted zone.
5. Comparing the impact energies of the variants, PC-GMAW exhibits a higher value of impact energy than the other three variants.
6. By reducing the heat input, the welding quality of the CMT-GMAW process is improved in terms of reduced distortions and spatter. This improved welding quality reduces post-production rework and thereby increases manufacturing efficiency. Thus, CMT welding is suitable for the fabrication of high-thickness joints at a low cost.

REFERENCES

[1] E. Taban, J. E. Gould, and J. C. Lippold, “Dissimilar friction welding of 6061-T6 aluminum and AISI 1018 steel: Properties and microstructural characterization,” Mater. Des., vol. 31, no. 5, pp. 2305–2311, 2010, https://doi.org/10.1016/j.matdes.2009.12.010

[2] W. S. Lee and C. F. Lin, “Impact properties and microstructure evolution of 304l stainless steel,” Mater. Sci. Eng. A, vol. 308, no. 1–2, pp. 124–135, 2001, https://doi.org/10.1016/S0921-5093(00)02024-4

[3] L. Shao and P. Yuan, “An immune detector based method for the diagnosis of compound faults in a petrochemical plant,” Trans. FAMENA, vol. 3, pp. 1–12, 2022, https://doi.org/10.21278/TOF.463033721

[4] E. Bajramoviü, D. Gaþo, and F. Islamoviü, “Behaviour of high-alloy steel welded joints of steam pipelines under the influence of temperature and exploitation time,” Trans. FAMENA, vol. 3, pp. 103–113, 2022, https://doi.org/10.21278/TOF.463039822

[5] Y. Kim, Y. Kim, and J. Kim, “DESIGN AND EXPERIMENTAL VALIDATION OF A CONTROL SYSTEM FOR DYNAMIC POSITIONING OF A SHUTTLE TANKER,” Trans. FAMENA, vol. 3, no. 2021, pp. 63–85, 1849, https://doi.org/10.21278/TOF.453029021

[6] J. Yan, M. Gao, and X. Zeng, “Study on microstructure and mechanical properties of 304 stainless steel joints by TIG, laser and laser-TIG hybrid welding,” Opt. Lasers Eng., vol. 48, no. 4, pp. 512–517, 2010, https://doi.org/10.1016/j.optlaseng.2009.08.009

[7] A. Ramaswamy, S. Malarvizhi, and V. Balasubramanian, “Effect of variants of gas metal arc welding process on tensile properties of AA6061-T6 aluminium alloy joints,” Int. J. Adv. Manuf. Technol., vol. 108, no. 9–10, pp. 2967–2983, 2020, https://doi.org/10.1007/s00170-020-05602-5

[8] J. Park, S. Kim, H. Moon, M. Kim, and D. Cho, “Effect of process parameters on root pass welding and analysis of microstructure in V-groove pulsed gas metal arc welding for mild steel,” pp. 1969–1985, 2020, https://doi.org/10.1007/s00170-020-05736-6

[9] C. L. Jenney and A. O’Brien, “Welding Handbook_Volume 1_WELDING SCIENCE AND TECHNOLOGY,” Am. Weld. Soc., vol. 1, p. 982, 1991.

[10] G. Küçüktürk, M. Tahta, H. Gürün, and I. Karaa, “Evaluation of the efffects of local heating on springback behaviour for AHSS docol 1400 sheet metal,” Trans. FAMENA, vol. 3, pp. 51–62, 2022, https://doi.org/10.21278/TOF.463037821

[11] N. P. Kumar, S. Arungalai Vendan, and N. Siva Shanmugam, “Investigations on the parametric effects of cold metal transfer process on the microstructural aspects in AA6061,” J. Alloys Compd., vol. 658, pp. 255–264, 2016, https://doi.org/10.1016/j.jallcom.2015.10.166

[12] G. Xu, J. Hu, and H. L. Tsai, “Three-dimensional modeling of arc plasma and metal transfer in gas metal arc welding,” Int. J. Heat Mass Transf., vol. 52, no. 7–8, pp. 1709–1724, 2009, https://doi.org/10.1016/j.ijheatmasstransfer.2008.09.018

[13] BibinJose, ManikandanManoharan, ArivazhaganNatarajan, N. Muktinutalapati, and G. M. Reddy, “Development of a low heat-input welding technique for joining thick plates of 250 grade maraging steel to fabricate rocket motor casings.” 2022, https://doi.org/10.1016/j.matlet.2022.132984

[14] P. Praveen, P. K. D. V. Yarlagadda, and M. J. Kang, “Advancements in pulse gas metal arc welding,” J. Mater. Process. Technol., vol. 164–165, pp. 1113–1119, 2005, https://doi.org/10.1016/j.jmatprotec.2005.02.100

[15] A. Liu, X. Tang, and F. Lu, “Study on welding process and prosperities of AA5754 Al-alloy welded by double pulsed gas metal arc welding,” Mater. Des., vol. 50, pp. 149–155, 2013, https://doi.org/10.1016/j.matdes.2013.02.087

[16] D. Srinivasan, P. Sevvel, I. John Solomon, P. Tanushkumaar, "A review on Cold Metal Transfer (CMT) technology of welding," Materials Today: Proceedings, Volume 64, Part 1, 2022, pp. 108-115, https://doi.org/10.1016/j.matpr.2022.04.016

[17] K. S. Derekar et al., “Effect of pulsed metal inert gas (pulsed-MIG) and cold metal transfer (CMT) techniques on hydrogen dissolution in wire arc additive manufacturing (WAAM) of aluminium,” Int. J. Adv. Manuf. Technol., vol. 107, no. 1–2, pp. 311–331, 2020, https://doi.org/10.1007/s00170-020-04946-2

[18] A. Mathivanan, A. Senthilkumar, and K. Devakumaran, “Pulsed current and dual pulse gas metal arc welding of grade AISI: 310S austenitic stainless steel,” Def. Technol., vol. 11, no. 3, pp. 269–274, 2015, https://doi.org/10.1016/j.dt.2015.05.006

[19] A. O. İrizalp, H. Durmuş, N. Yüksel, and İ. Türkmen, “Cold metal transfer welding of AA1050 aluminum thin sheets,” Rev. Mater., vol. 21, no. 3, pp. 615–622, 2016, https://doi.org/10.1590/S1517-707620160003.0059

[20] C. G. Pickin, S. W. Williams, and M. Lunt, "Characterisation of the cold metal transfer (CMT) process and its application for low dilution cladding," J. Mater. Process. Technol., vol. 211, no. 3, pp. 496–502, 2011, https://doi.org/10.1016/j.jmatprotec.2010.11.005

[21] P. Kah, R. Suoranta, and J. Martikainen, "Advanced gas metal arc welding processes," Int. J. Adv. Manuf. Technol., vol. 67, no. 1–4, pp. 655–674, 2013, https://doi.org/10.1007/s00170-012-4513-5

[22] G. Liu et al., "Analysis of microstructure, mechanical properties, and wear performance of NiTi alloy fabricated by cold metal transfer based wire arc additive manufacturing," J. Mater. Res. Technol., vol. 20, pp. 246–259, 2022, https://doi.org/10.1016/j.jmrt.2022.07.068

[23] L. Dong, Z. Shi, Y. Zhang, S. Wang, Q. Wang, and L. Liu, "Microstructure and sulfide stress corrosion cracking of the Inconel 625/X80 weld overlay fabricated by cold metal transfer process," Int. J. Hydrogen Energy, vol. 47, no. 67, pp. 29113–29130, 2022, https://doi.org/10.1016/j.ijhydene.2022.06.210

[24] J. Feng, H. Zhang, and P. He, "The CMT short-circuiting metal transfer process and its use in thin aluminium sheets welding," Mater. Des., vol. 30, no. 5, pp. 1850–1852, 2009, https://doi.org/10.1016/j.matdes.2008.07.015

[25] H. T. Zhang, J. C. Feng, and P. He, "Interfacial phenomena of cold metal transfer (CMT) welding of zinc coated steel and wrought aluminium," Mater. Sci. Technol., vol. 24, no. 11, pp. 1346–1349, 2008, https://doi.org/10.1179/174328407X213152

[26] K. Furukawa, "New CMT arc welding process – welding of steel to aluminium dissimilar metals and welding of super-thin aluminium sheets," Weld. Int., vol. 20, no. 6, pp. 440–445, 2006, https://doi.org/10.1533/wint.2006.3598

[27] A. Schierl and Bruckner, "The CMT Process a Revolution in welding technology." in Benefits of new methods and trends in welding to economy, productivity and quality welding in the world -, 49; 38, London, 2005, ISSN: 0043-2288.

[28] Z. Sun, Y. Lv, B. Xu, Y. Liu, J. Lin, and K. Wang, "Investigation of droplet transfer behaviours in cold metal transfer (CMT) process on welding Ti-6Al-4V alloy," Int. J. Adv. Manuf. Technol., vol. 80, no. 9–12, pp. 2007–2014, 2015, https://doi.org/10.1007/s00170-015-7197-9

[29] M. Grzybicki and J. Jakubowski, "Comparative tests of steel car body sheet welds made using CMT and MIG/MAG methods," Weld. Int., vol. 27, no. 8, pp. 610–615, 2013, https://doi.org/10.1080/09507116.2011.606147

[30] J. C. Dutra, R. H. Gonçalves e Silva, and C. Marques, "Melting and welding power characteristics of MIG–CMT versus conventional MIG for aluminium 5183," Weld. Int., vol. 29, no. 3, pp. 181–186, 2015, https://doi.org/10.1080/09507116.2014.932974

[31] M. R. U. Ahsan, Y. R. Kim, C. H. Kim, J. W. Kim, R. Ashiri, and Y. D. Park, "Porosity formation mechanisms in cold metal transfer (CMT) gas metal arc welding (GMAW) of zinc coated steels," Sci. Technol. Weld. Join., vol. 21, no. 3, pp. 209–215, 2016, https://doi.org/10.1179/1362171815Y.0000000084

[32] A. Benoit, P. Paillard, T. Baudin, V. Klosek, and J. B. Mottin, "Comparison of four arc welding processes used for aluminium alloy cladding," Sci. Technol. Weld. Join., vol. 20, no. 1, pp. 75–81, 2015, https://doi.org/10.1179/1362171814Y.0000000257

[33] HaoyuCai, LianyongXu, LeiZhao, YongdianHan, HongningPang, and WeiChenab, "Cold metal transfer plus pulse (CMT+P) welding of G115 steel: Mechanisms, microstructure, and mechanical properties." 2022, https://doi.org/https://doi.org/10.1016/j.msea.2022.143156

Submitted: 26.11.2022

Accepted: 24.5.2023

Karthick K*
Assistant Professor in Mechanical Engineering,
KGiSL Institute of Technology,
Coimbatore, India

Magudeeswaran G
magudeeswaran@yahoo.com
Professor of Mechanical Engineering,
PSNA College of Engineering and Technology, Dindigul, India

*Corresponding author:
karthick32mech@gmail.com